

# Crystal Structure and Functional Characterization of the Complement Regulator Mannose-binding Lectin (MBL)/Ficolin-associated Protein-1 (MAP-1)\*<sup>§</sup>

Received for publication, May 30, 2012, and in revised form, July 6, 2012. Published, JBC Papers in Press, August 1, 2012, DOI 10.1074/jbc.M112.386680

Mikkel-Ole Skjoed<sup>†1,2</sup>, Pietro Roversi<sup>§1</sup>, Tina Hummelshøj<sup>‡</sup>, Yaseelan Palarasah<sup>¶</sup>, Anne Rosbjerg<sup>‡</sup>, Steven Johnson<sup>§</sup>, Susan M. Lea<sup>§</sup>, and Peter Garred<sup>‡</sup>

From the <sup>†</sup>Laboratory of Molecular Medicine, Department of Clinical Immunology, Rigshospitalet, Faculty of Health Sciences, University of Copenhagen, DK 2100 Copenhagen, Denmark, <sup>§</sup>Sir William Dunn School of Pathology, University of Oxford, OX1 3RE Oxford, United Kingdom, and <sup>¶</sup>Research Unit of Cancer and Inflammation, University of Southern Denmark, DK5000 Copenhagen, Denmark, and Institute for Inflammation Research, Rigshospitalet, DK2100 Copenhagen, Denmark

**Background:** MAP-1 is a novel member of the lectin complement pathway.

**Results:** We present the crystal structure of MAP-1 and show that it inhibits central complement factors and interacts with MBL and ficolin at nM affinities.

**Conclusion:** MAP-1 is a Ca<sup>2+</sup>-dependent homo-dimer molecule and a key complement regulator.

**Significance:** Structural and functional knowledge of MAP-1 provide important insight to the biology of the complement system.

The human lectin complement pathway activation molecules comprise mannose-binding lectin (MBL) and ficolin-1, -2, and -3 in complex with associated serine proteases MASP-1, -2, and -3 and the non-enzymatic small MBL associated protein or sMAP. Recently, a novel plasma protein named MBL/ficolin-associated protein-1 (MAP-1) was identified in humans. This protein is the result of a differential splicing of the *MASPI* gene and includes the major part of the heavy chain but lacks the serine protease domain. We investigated the direct interactions of MAP-1 and MASP-3 with ficolin-3 and MBL using surface plasmon resonance and found affinities around 5 nM and 2.5 nM, respectively. We studied structural aspects of MAP-1 and could show by multi-angle laser light scattering that MAP-1 forms a calcium-dependent homodimer in solution. We were able to determine the crystal structure of MAP-1, which also contains a head-to-tail dimer ~146 Å long. This structure of MAP-1 also enables modeling and assembly of the MASP-1 molecule in its entirety. Finally we found that MAP-1 competes with all three MASPs for ligand binding and is able to mediate a strong dose-dependent inhibitory effect on the lectin pathway activation, as measured by levels of C3 and C9.

The complement system mediates inflammatory and immunological host responses toward pathogens. Three biochemical pathways activate the complement system: the classical, the alternative, and the lectin complement pathway, respectively (1, 2). Activation of these cascades results in a massive amplification of the response, leading to recognition of pathogens, release of inflammatory and chemotactic mediators, recruitment of inflammatory cells, vasodilation, and elimination of invading microorganisms. In addition, complement facilitates the clearance of dead or altered self-antigens, such as apoptotic cells and cellular debris. Multiple regulatory proteins influence virtually every stage of the response, preventing excess complement activation and collateral damage of host cells (3). However, genetic deficiencies in the regulators or excessive activation of complement in response to certain pathological conditions can destroy tissue homeostasis and have been associated with a number of autoimmune diseases (3–6).

The lectin complement pathway plays an important role in innate immunity and in the clearance of foreign and self-antigens, and it has also been shown to have a central role in the pathophysiology of ischemia reperfusion injury (7–9). Four recognition molecules have been firmly established in the lectin complement pathway: mannose-binding lectin (MBL),<sup>3</sup> and the three ficolins, labeled 1, 2, and 3 (10). They bind glycosylated structures on different classes of microorganisms and are also involved in sequestration and removal of dying host cells (11, 12). Three MBL/ficolin-associated serine proteases have been described (MASP-1, MASP-2, and MASP-3) and a protein lacking a serine protease domain

\* This work was supported by the National Research Council for Health and Disease in Denmark, the Capital Region of Denmark, The Novo Nordisk Research Foundation, The Sven Andersen Research Foundation, and the John and Birthe Meyer Foundation and Rigshospitalet.

<sup>§</sup> This article contains supplemental Movie 1.

The atomic coordinates and structure factors (code 4aqb) have been deposited in the Protein Data Bank, Research Collaboratory for Structural Bioinformatics, Rutgers University, New Brunswick, NJ (<http://www.rcsb.org/>).

<sup>1</sup> Both authors contributed equally and should be regarded as joint first authors.

<sup>2</sup> To whom correspondence should be addressed: Laboratory of Molecular Medicine, Dept. of Clinical Immunology, Section 7631, Rigshospitalet, Blegdamsvej 9, DK 2100 Copenhagen, Denmark. Tel.: 45-35457631; Fax: 45-35398766; E-mail: moskjoedt@gmail.com.

<sup>3</sup> The abbreviations used are: MBL, mannose-binding lectin; MASP, MBL/ficolin-associated serine protease; sMAP/Map19, small MBL/ficolin-associated protein/19-kDa MBL-associated protein; MAP-1, MBL/ficolin-associated protein 1; SCR/CCP, short consensus repeats/complement control protein; CUB, C1r/C1s, Urchin-EGF, bone morphogenetic protein; SP, serine protease; Bis-Tris, 2-[bis(2-hydroxyethyl)amino]-2-(hydroxymethyl)propane-1,3-diol.

## Structure and Function of MAP-1

named small MBL associated protein or sMAP (also known as MAP19) (13). MASP-1 and MASP-3 are alternative spliced forms of the *MASP1* gene; they share five domains but have unique protease domains. MASP-2 is encoded by a separate gene, and present consensus places it as the main initiator of the lectin complement pathway; upon activation, MASP-2 cleaves complement factors C4 and C2, leading to the formation of C3 convertases that amplify and carry the response further (14). The functions of the other MASPs are less well understood; MASP-1 appears to play a role as an amplifier of complement activation (15, 16) and mediates direct activation of the alternative pathway component factor D in mice (17); additionally, MASP-1-mediated complement cross-talk with the coagulation and the kallikrein systems has been reported (18, 19). No conclusive biological function has yet been attributed to MASP-3 and sMAP. However, two independent studies have shown that mutations in the part of the *MASP1* gene encoding the serine protease domains of MASP-3 influence embryogenesis and are associated with developmental disorders (20, 21). The major biological function of the *MASP1* gene products could, therefore, be linked to elements outside of the complement system and innate immunity as such. Recently, a novel member of the lectin complement pathway called MAP-1 (for MBL/ficolin-associated protein 1; alternative name, MAP44 or *MASP1* isoform 3) was described (22, 23). Like MASP-1 and MASP-3, the non-enzymatic MAP-1 is also derived from the *MASP1* gene (located on chromosome 3q27-q28) through differential splicing. Except for 15 C-terminal residues, MASP-1 and MASP-3 contain identical heavy chains comprised of two CUBs (C1r/C1s, urchin-EGF, bone morphogenetic protein) separated by an epidermal growth factor (EGF) domain and followed by two CCP/SCR (complement control protein/short consensus repeats) domains. The light chain of MASP-1 and MASP-3 contains the serine protease domain, which is different in the two proteins. MAP-1 comprises the major part of the heavy chain including the two CUB domains, the EGF, and the first of two SCR domains. Additionally, the molecule has a unique 17-residue C-terminal end but lacks a serine protease domain. MAP-1 circulates in complexes with MBL and the plasma ficolins and inhibits C4 activation (22–24). The tissue distribution profile is very different for MAP-1 compared with the other lectin complement pathway members. A high expression is observed in myocardial fibers, in skeletal muscle tissue, and to some degree in liver and nerve tissues (23). The mechanisms behind the regulation of the *MASP1* gene expression remain unclear.

Separate crystal structures for constructs corresponding to the shared part of the heavy chain (25) and the catalytic domain of the MASP-1 molecule have been published (26). Here we describe the first crystal structure of a complete MAP-1 molecule and present interaction affinities with MBL and ficolin-3. We also show that MAP-1 has a significant dose-dependent inhibitory effect on the lectin complement pathway activation of the central complement factor C3 and downstream formation of the terminal complement complex.

**TABLE 1**

### MAP-1 data collection and refinement statistics

Values in parentheses are for highest resolution shell. r.m.s.d., root mean square deviation.

Data acquisition	
Beamline, $\lambda$ (Å)	ESRF ID14-4, 0.97930
Space group (Z)	P4 <sub>3</sub> 22 (8)
Molecules/asymmetric unit (asu)	1
Cell dimensions <i>a, b, c</i> (Å)	94.1, 94.1, 242.7
Observations	18,636 (1,999)
Unique observations	7,844 (512)
Resolution (Å)	94–4.2 (5.2–4.2)
$R_{\text{sym}}$ or $R_{\text{merge}}$	0.28 (0.55)
$I/\sigma$	8.7 (2.8)
Completeness (%)	93.5 (95.2)
Redundancy	3.6 (3.9)
Refinement	
$R_{\text{work}}/R_{\text{free}}$	0.28/0.30
No. atoms	2,914
Protein	2,792
Ligand/ion/waters	6 Ca <sup>+2</sup> ions
r.m.s.d. bond lengths (Å)	0.006
r.m.s.d. bond angles (°)	1.02

## EXPERIMENTAL PROCEDURES

### Expression and Purification of Recombinant Proteins

Recombinant proteins (rMAP-1, rMASP-3, rMBL, and rfcolin-3) were all expressed in the CHO DG44 cell line using the CHO CD1 serum-free medium (Cambrex) as described previously (23, 24). Recombinant MBL was affinity-purified by mannan-agarose affinity chromatography essentially as described by Vorup-Jensen *et al.* (27). The other proteins were antibody affinity-purified with mAb 20C4 (MAP-1), mAb 8B3 (MASP-3), and mAb FCN334 (ficolin-3) as previously described (24). Collectin-11 was purchased from R&D Systems, Inc. (CL-K1/COLEC11; Abingdon, Oxford, UK).

### Size Exclusion Chromatography Multi-angle Laser Light Scattering

Size exclusion chromatography was performed on a Superose 6 10/30 column (GE Healthcare) equilibrated in 50 mM Tris-HCl, pH 7.5, 150 mM NaCl at 0.4 ml/min. Protein samples were supplemented with either 2 mM CaCl<sub>2</sub> or 10 mM EDTA before injection. The column was followed in-line by a Dawn Heleos-II light scattering detector (Wyatt Technologies) and an Optilab-Rex refractive index monitor (Wyatt Technologies). Molecular mass calculations were performed using ASTRA 5.3.4.14 (Wyatt Technologies) assuming a refractive index increment (dn/dc) value of 0.186 ml/g.

### MAP-1 Structure Determination

**Crystallization**—Tetragonal MAP-1 crystals were grown at 21 °C by the sitting drop vapor diffusion by mixing 280 nl of MAP-1 at ~2.5 mg/ml (protein in Tris-buffered saline, pH 7.2, + 2 mM CaCl<sub>2</sub>) with 120 nl of 0.2 M calcium acetate, 0.1 M sodium cacodylate, pH 6.5, 40% w/v PEG 400. The drops were set up with an Oryx Nano crystallization robot.

**Diffraction**—The crystals diffracted on beamline ID14-4 at the European Synchrotron Radiation Facility on 11 April 2011. They were anisotropically truncated and sharpened to 4.2 Å with the Anisotropy Server. For details of data statistics, see Table 1.

**Structure Solution**—The structure was determined by molecular replacement in two stages. First, the CUB<sub>1</sub>-EGF-CUB<sub>2</sub> portion was located using the program Phaser using the corresponding MASP-1 portion as a search model (PDB ID 3DEM, residues 23–297). Then, the C-terminal SCR<sub>1</sub> (CCP<sub>1</sub>) domain was located with program Molrep, searching with the first SCR domain of the MASP-1 SCR<sub>1</sub>-SCR<sub>2</sub>-SP construct (residues 299–364, PDB ID 3GOV) in the presence of the already placed CUB<sub>1</sub>-EGF-CUB<sub>2</sub>.

**Refinement**—Refinement of the structure was performed with the program autoBUSTER using the 3DEM and 3GOV structures as target restraints and with thermal motion modeled with one translation libration screw (TLS) body per domain. The GlcNAc<sub>2</sub>Man<sub>3</sub> portion of the N-linked glycans at Asn-49 and Asn-178 were modeled in the density after being generated by the GlyProt server. Details of the refinement are presented in Table 1. The structure was deposited in the PDB with accession code 4aqb.

### Surface Plasmon Resonance Spectroscopy Measurements

The data were collected on a BiaCore 3000 instrument. All coupling was effected at 55  $\mu$ l/min onto a Sensor Chip CM5 (GE Healthcare) activated with 40  $\mu$ l of a 1:1 mixture of 0.1 M N-hydroxysuccinimide (NHS) and 0.4 M 1-ethyl-3-(3-dimethylpropyl)-carbodiimide (EDC) stock solutions. Channel 1 was 60  $\mu$ l of a BSA solution obtained mixing 77.5  $\mu$ l of 10 mM NaOAc, pH 4.0, with 22.5  $\mu$ l of a stock solution of 0.133 mg/ml BSA in water. Channel 3 was 40  $\mu$ l of a solution obtained mixing 98  $\mu$ l of 10 mM NaOAc, pH 4.0, with 2  $\mu$ l of a stock solution of 3.3 mg/ml ficolin-3 in water. The coupling resulted in the immobilization of 10,700 resonance units. Channel 4 was 60  $\mu$ l of a solution obtained mixing 90  $\mu$ l of 10 mM NaOAc, pH 4.0, with 10  $\mu$ l of a stock solution of 1.26 mg/ml MBL in water. The coupling resulted in the immobilization of 2900 resonance units.

Chip inactivation was then effected by 100  $\mu$ l of 1 M ethanolamine hydrochloride, pH 8.5, flowing over each channel at 20  $\mu$ l/min. The chip was then equilibrated in the running buffer: 145 mM NaCl, 1 mM CaCl<sub>2</sub>, 50 mM triethanolamine hydrochloride pH 7.4, 0.005% surfactant P20, 10 mM D-(+)-mannose. All measurements were conducted at a constant flow rate of 20  $\mu$ l/min. For injections, 60  $\mu$ l of ligand were flowed over the channels of the CM5 chip. Dissociation was measured for 300 s. After each injection and dissociation, the chip was washed with 10  $\mu$ l of 1 M NaCl, 10 mM EDTA and then re-equilibrated for 100 s in running buffer.

### Interactions of MASP-3

A 122 nM solution of MASP-3 was prepared by mixing 3  $\mu$ l of a solution 9.76  $\mu$ M MASP-3, 2 mM CaCl<sub>2</sub>, and 20 mM HEPES, pH 7.2, into 237  $\mu$ l of running buffer. A series of 1:1 dilutions in the same buffer were then prepared to give 61, 30.5, 15.25, and 7.625 nM MASP-3 solutions.

### Interactions of MAP-1

A 144 nM solution of MAP-1 was prepared by mixing 1  $\mu$ l of a solution 173  $\mu$ M MAP-1, 2 mM CaCl<sub>2</sub>, and 20 mM HEPES, pH 7.2, into 239  $\mu$ l of running buffer. A series of 1:1 dilutions in the same buffer were then prepared to give 72, 36, 18, 9, and 4.5 nM MAP-1 solutions.

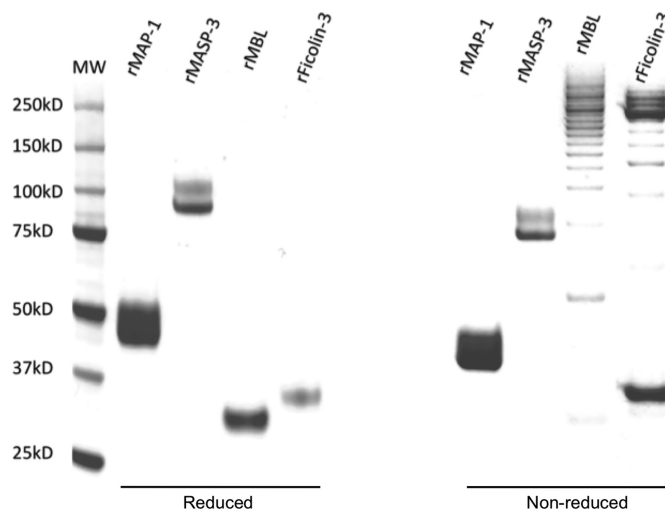


FIGURE 1. **Recombinant proteins.** Shown are 4–12% Bis-Tris SDS-PAGE and Coomassie staining of recombinant expressed and purified MAP-1, MASP-3, MBL, and ficolin-3. The expression system was CHO DG44; left, reduced samples; right, non-reduced.

### MAP-1/MASP Competition Assays

Recombinant ficolin-3 bound to acetylated bovine serum albumin was used as a ligand partner for the binding of MAP-1 and the MASPs essentially as described previously (16). Briefly, acetylated BSA was immobilized in microtiter plates at 5  $\mu$ g/ml followed by incubation of r ficolin-3 at 0.5  $\mu$ g/ml. Serial dilutions of rMAP-1 together with rMASP-1, -2, or -3 were then coincubated on the acetylated BSA/r ficolin-3 matrix for 2 h at 20 °C. Binding of MASP-1 and -3 was measured with 2  $\mu$ g/ml concentrations of an in-house monoclonal mouse antibody (MASP1/3 F3–46) that reacts with a common MASP-1/-3 epitope but does not cross-react with MAP-1. MASP-2 binding was detected with the 8B5 monoclonal rat antibody at 2  $\mu$ g/ml (catalog #HM2190, Hycult Biotech, Uden, The Netherlands). Secondary antibodies were HRP-conjugated rabbit anti-mouse or HRP-conjugated rabbit anti-rat (P0260 or P0450, both from Dako, Glostrup, Denmark). The plates were developed with ortho-phenylenediamine (OPD)/H<sub>2</sub>O<sub>2</sub> substrate as recommended by the manufacturer (Dako).

### Complement Activation Assays

The complement activation assays were conducted as described previously (23, 28). Briefly, microtiter plates were coated with 10  $\mu$ g/ml mannan, and after blocking rMBL was applied at a concentration of 0.4  $\mu$ g/ml. Sodium polyanethole sulfonate was used to block interference from the classical and alternative pathway as described by Palarasah *et al.* (29) to specifically assess the influence of the MBL pathway by reconstitution of homozygous MBL defect serum (genotype D/D) serum with rMBL (30). Activation and deposition of endogenous C3 and C9 was measured with specific monoclonal antibodies against these factors as described previously (28).

## RESULTS

**Purification of Recombinant Proteins**—Fig. 1 shows the purity of recombinant MAP-1, MASP-3, MBL, and ficolin-3. A single protein band represents MBL and ficolin-3 under reduc-



## Structure and Function of MAP-1

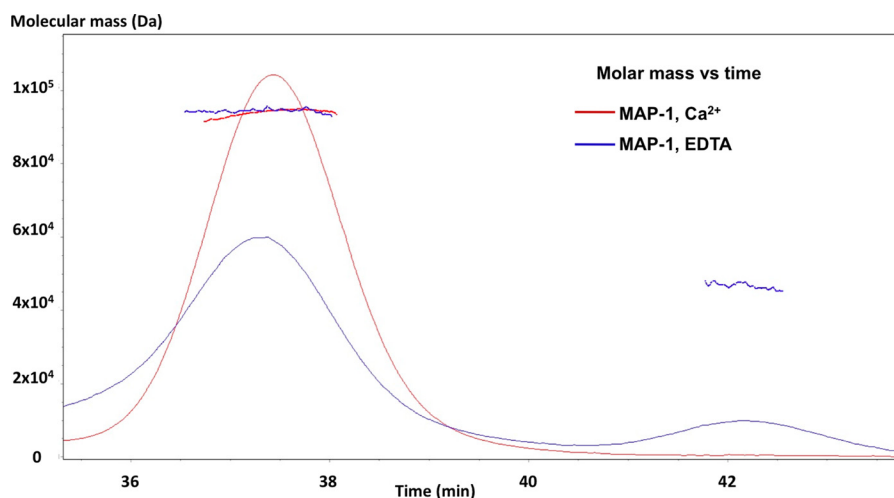


FIGURE 2. **MAP-1 molecular mass determination.** Multi-angle laser light scattering of recombinant MAP-1 is shown. The red curve shows rMAP-1 in TBS/2 mM  $\text{Ca}^{2+}$ . The blue curve reflects the same setup with TBS/10 mM EDTA. The latter curve shows that the dimer peak is weaker, and a monomer peak appears. Calculated mass across each peak is shown. The masses are 47 and 94 kDa for the monomer and dimer, respectively.

ing conditions. *N*-Glycosylations of rMAP-1 and rMASP-3 produce the smeared/double band pattern as reported previously (16, 24). Non-reduced SDS-PAGE reflects the disulfide bridge-dependent oligomerization pattern seen for MBL and ficolin-3. Because of intrachain disulfide bridges in rMAP-1 and rMASP-3, the molecules migrate a bit further through the gel matrix under non-reducing conditions.

**Structural Data**—Non-covalent calcium interactions mediate the homodimerization of rMAP-1. We analyzed rMAP-1 under physiological calcium concentrations by multi-angle laser light scattering and found that it elutes as a peak with a molecular mass of around 94 kDa corresponding to a dimer (Fig. 2). When calcium-chelating conditions (EDTA) were introduced to the analysis, we observed a reduction in the dimer peak and the appearance of a peak with a mass around 47 kDa corresponding to a monomer.

We grew tetragonal MAP-1 crystals under the conditions described under “Experimental Procedures.” The crystal analysis shows a molecule with an elongated linear shape  $\sim 146$  Å in length. At 5 Å resolution, we cannot reliably model differences with respect to the MASP-1 construct crystallized earlier (PDB ID 3DEM), although main chain density is visible in the MAP-1 crystal for the loop 146–150, which was not modeled in PDB ID 3DEM. Three more  $\text{Ca}^{+2}$  sites were also modeled on the surface. The core pentasaccharide of *N*-linked glycans at Asn-49 and Asn-178 is visible in the density and was modeled as  $\text{GlcNAc}_2\text{Man}_3$  (Fig. 3A). The MAP-1 crystals contain the same CUB-mediated dimer observed in the MASP-1 CUB<sub>1</sub>-EGF-CUB<sub>2</sub> crystals (PDB ID 3DEM) arranged around a crystallographic 2-fold axis of space group  $\text{P4}_322$ . Fig. 3B illustrates the MAP-1 dimer overlaid with the MASP-1 dimer from PDB ID 3DEM. A movie of the MAP-1 monomer rotating around its long axis can be displayed in supplemental data S1.

The MAP-1 structure allows for the first time the modeling of MASP-1 in its entirety; Fig. 3C illustrates two views of a model for the MASP-1 dimer obtained by overlaying residues 26–297 from PDB ID 3DEM and residues 299–364 of PDB ID 3GOV onto the corresponding residues of MAP-1 and then

assembling the two overlaid halves of MASP-1 together. The full MASP-1 molecule is gently curved and measures  $\sim 206$  Å from head to tail. The MASP-1 dimer appears to be flat, and the distance between the two SP heads is  $\sim 330$  Å.

**Interactions with MBL and Ficolin-3**—We assessed the binding properties of rMASP-3 and rMAP-1 to rMBL and rFicolin-3 by surface plasmon resonance spectroscopy using the Biacore platform. rMBL and rFicolin-3 were immobilized on the sensor chip, and rMASP-3 and rMAP-1 were applied in the fluid phase. We also tried to immobilize collectin-11 onto a sensor chip, but we were not able to bind this protein to the chip matrix despite several attempts with different conditions. BSA immobilized to a sensor chip served as background control. The sensorgrams were fitted using a 1:1 Langmuir binding model (Fig. 4) yielding  $K_d$  estimates for all interactions studied in the 2–7 nM range, consistent with affinities previously reported for interactions involving these domains (31–33). We found that rMASP-3 interacts with MBL and ficolin-3 with dissociation constants  $K_d$  of 3 and 2 nM, respectively ( $k_{\text{on}} = 1 \cdot 10^5 \text{ M}^{-1}\text{s}^{-1}$  and  $k_{\text{off}} = 3 \cdot 10^{-4} \text{ s}^{-1}$  for MBL and  $k_{\text{on}} = 9 \cdot 10^4 \text{ M}^{-1}\text{s}^{-1}$  and  $k_{\text{off}} = 2 \cdot 10^{-4} \text{ s}^{-1}$  for ficolin-3). rMAP-1 interacts with an affinity  $K_d$  of 5 nM with MBL and 7 nM with ficolin-3 ( $k_{\text{on}} = 2 \cdot 10^5 \text{ M}^{-1}\text{s}^{-1}$  and  $k_{\text{off}} = 7 \cdot 10^{-4} \text{ s}^{-1}$  for MBL and  $k_{\text{on}} = 1 \cdot 10^5 \text{ M}^{-1}\text{s}^{-1}$  and  $k_{\text{off}} = 8 \cdot 10^{-4} \text{ s}^{-1}$  for ficolin-3).

**MAP-1/MASP Competition**—The direct competition between MAP-1 and the MASPs for ligand binding was evaluated on a ficolin-3 binding matrix. Incubation of rMASP-1, -2, and -3 in the absence of rMAP-1 resulted in a concentration-dependent MASP binding shown in Fig. 5. Co-incubation with rMAP-1 caused a significant decrease in the MASP-1, -2, and -3 binding to ficolin-3 in a MAP-1 dose-dependent manner. Intermediate MASP inhibition was seen with 25 nM rMAP-1, and an almost complete MASP binding inhibition was observed with co-incubation of 667 nM rMAP-1 (Fig. 5). No significant effect on the MASP binding was observed in MAP-1 concentrations below 1 nM (data not shown).

**Complement Inhibition**—We assessed the dose-dependent effect of rMAP-1 on the endogenous serum capacity to activate and deposit the central complement factor C3 and the

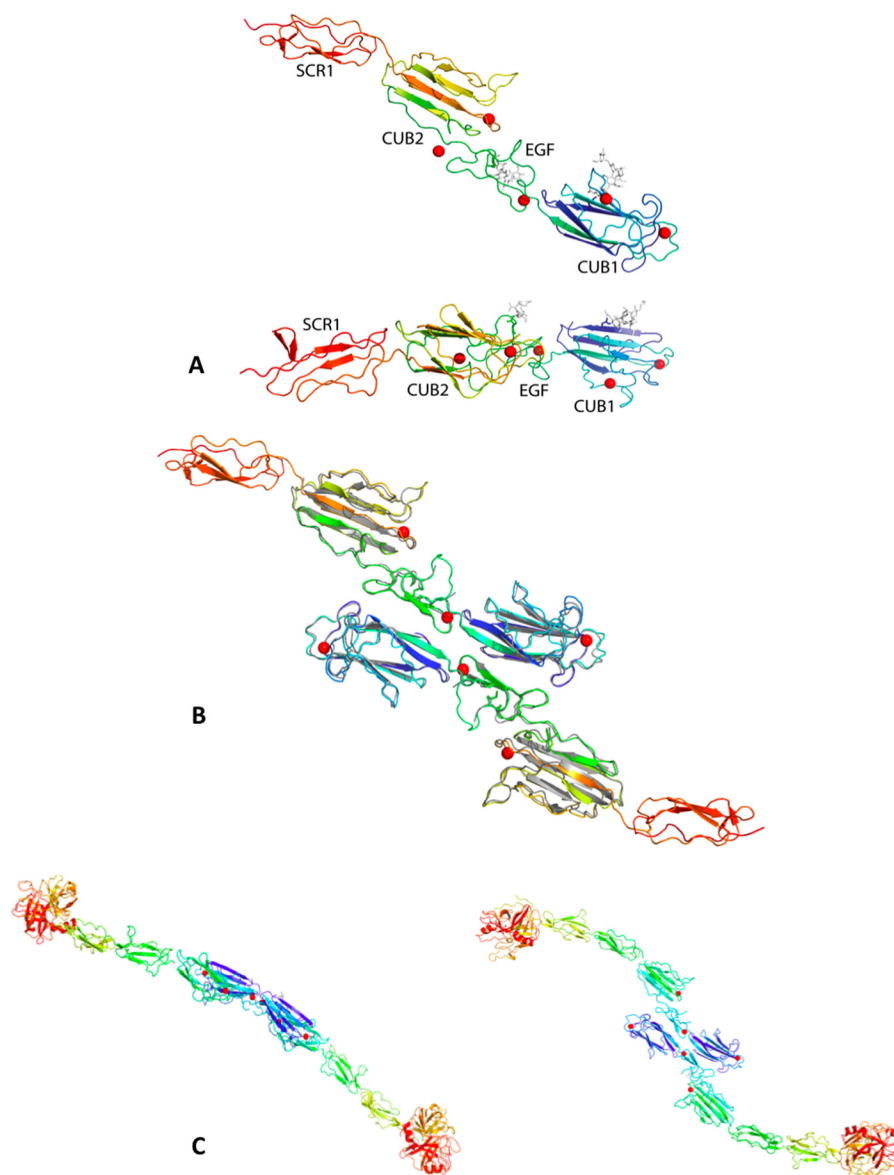


FIGURE 3. **Structural models of MAP-1 and MASP-1.** *A*, MAP-1 monomers are shown and are colored *blue to red* from the N to C terminus.  $\text{Ca}^{+2}$  ions involved in the dimerization are represented as *red spheres*, and *N*-linked glycans at Asn-49 and Asn-178 are represented in *gray sticks*. The two views are related by a  $90^\circ$  rotation around the horizontal axis. *B*, the MAP-1 dimer, colored as in *A*, overlaid onto the MASP-1 CUB<sub>1</sub>-EGF-CUB<sub>2</sub> dimer from PDB ID 3DEM (*gray*). *C*, shown are two views of a model for the entire MASP-1 dimer, colored *blue to red* from the N to C termini. It was obtained by overlaying onto the MAP-1 dimer the two portions of the MASP-1 molecule from PDB IDs 3GOV (CUB<sub>1</sub>-EGF-CUB<sub>2</sub>) and 3DEM (SCR<sub>1</sub>-SCR<sub>2</sub>-SP). The two views are rotated by  $90^\circ$  around the horizontal direction.

terminal complement component C9. Serum from an individual with a homozygous MBL defect was reconstituted with  $0.4 \mu\text{g/ml}$  rMBL bound to mannan. The activation of endogenous C3 and C9 was subsequently assessed with monoclonal antibodies. A serum dose-dependent activation and deposition of C3 and C9 was observed for the MBL reconstituted serum, whereas no deposition was evident without application of rMBL (Fig. 6A). When rMAP-1 was preincubated on the bound rMBL before the application of the MBL defect serum, we observed a strong inhibitory effect on the activation of both C3 and C9. A significant inhibition was seen already from a MAP-1 concentration of  $0.3 \text{ nM}$ , and an almost complete inhibition of the C3 and C9 deposition was observed from  $8 \text{ nM}$ . No further effect on the comple-

ment inhibition was observed in concentrations above  $25 \text{ nM}$  (Fig. 6, *B* and *C*).

## DISCUSSION

This study presents the first crystal structure of the recently described MAP-1. The structure of the first three domains fits well with the previous published CUB<sub>1</sub>-EGF-CUB<sub>2</sub> of MASP-1/MASP-3 (25). The MAP-1 structure also includes the structure of the junction region between the CUB<sub>2</sub> and the SCR<sub>1</sub>. The 17 C-terminal residues that are unique to MAP-1 are disordered in the crystal. The complete structure shows an elongated dimer molecule of  $146 \text{ \AA}$  in length that includes 12 calcium interaction sites and two *N*-linked GlcNAc<sub>2</sub>Man<sub>3</sub> glycans at positions Asn-49 and Asn-178. We were also able to model

## Structure and Function of MAP-1

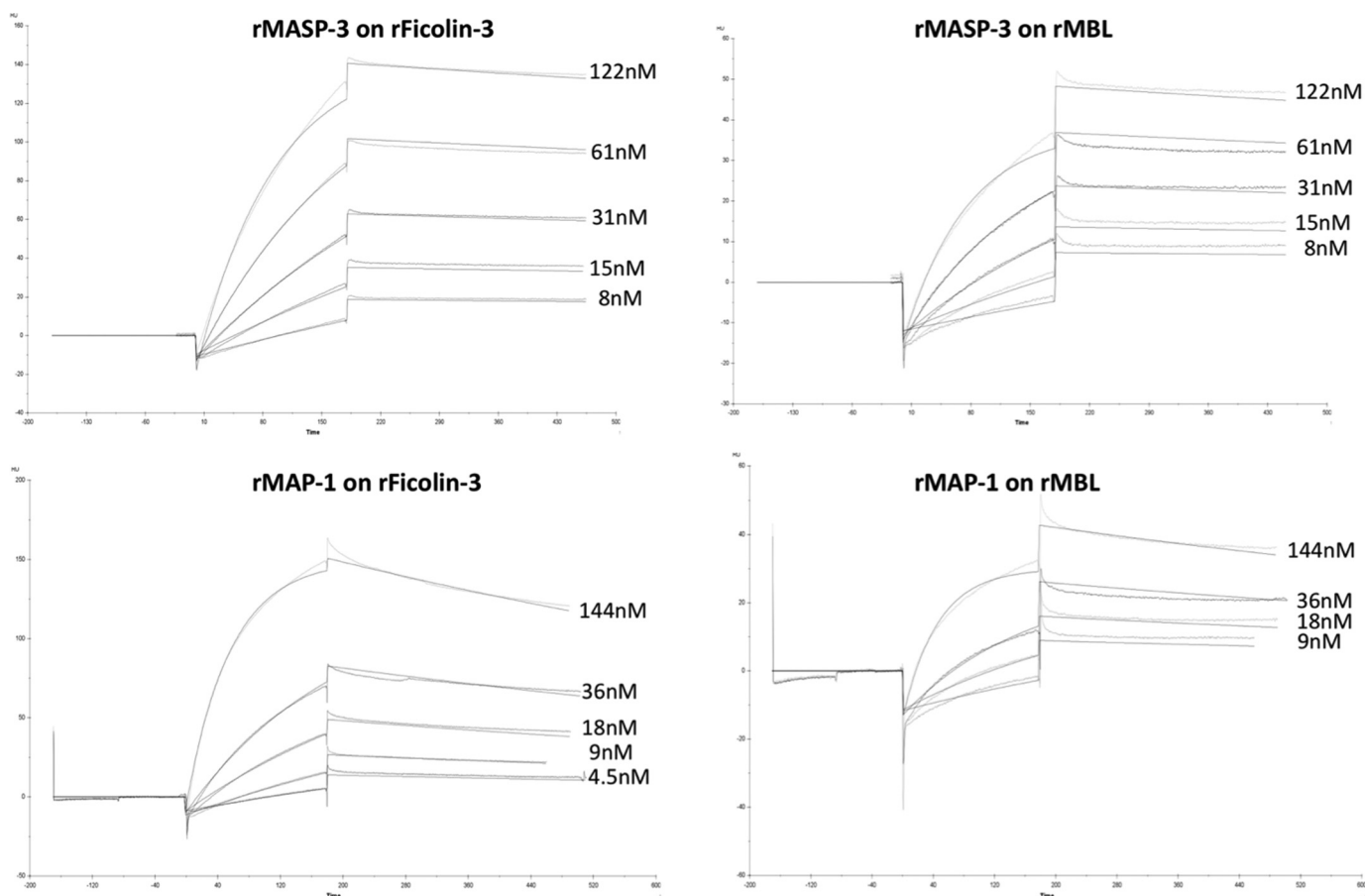


FIGURE 4. **Sensorgrams of the interactions between MASP-3 and MAP-1 with ficolin-3 and MBL.** All measurements were conducted at a constant flow rate of 20  $\mu\text{l}/\text{min}$  and with 60- $\mu\text{l}$  injections of the ligands. Recombinant ficolin-3 was immobilized to the chip with 2  $\mu\text{l}$  of a stock solution of 3.3 mg/ml in MBL and was immobilized with 10  $\mu\text{l}$  of a stock solution of 1.26 mg/ml MBL in water. The *black curves* represent the simultaneous fitting over all concentrations of the  $k_{\text{on}}/k_{\text{off}}$  using a 1:1 Langmuir binding model.

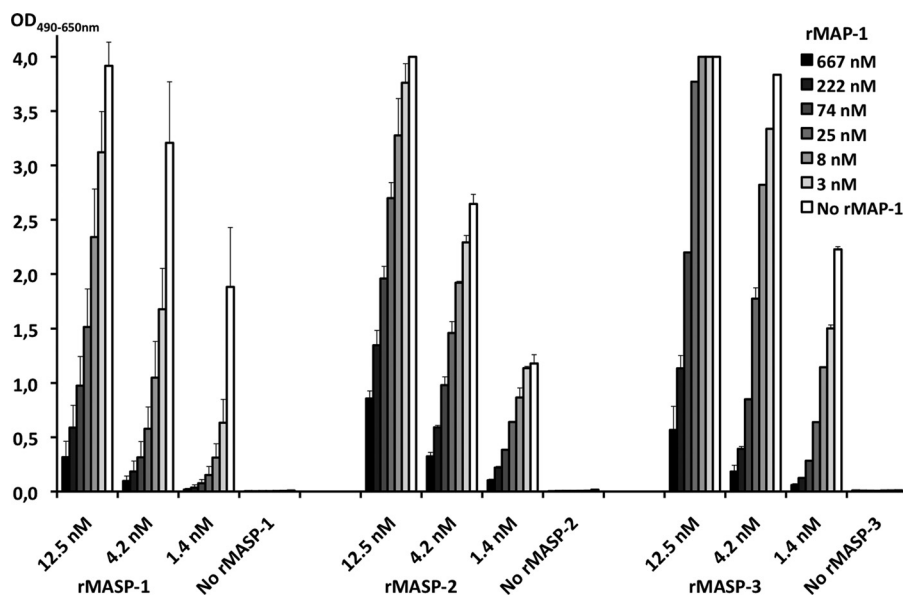


FIGURE 5. **Competition between MAP-1 and MASP-1, -2, and -3 for the binding to ficolin-3.** rMAP-1 was co-incubated together with rMASP-1, -2, or -3 in different concentrations on acetylated BSA-bound ficolin-3. The binding of rMASP-1, -2, and -3 was measured with specific monoclonal antibodies that do not cross-react with MAP-1. *Error bars* indicate two times the S.D. of double determinations.

the structure of a complete MASP-1 dimer by overlaying onto our MAP-1 dimer the two portions of the MASP-1 molecule from PDB IDs 3GOV (CUB<sub>1</sub>-EGF-CUB<sub>2</sub>) and 3DEM (SCR<sub>1</sub>-

SCR<sub>2</sub>-SP). The model shows MASP-1 as a gently curved molecule of  $\sim 206$  Å from head to tail. The modeled MASP-1 dimer appears to be flat, and the distance between the two SP heads is

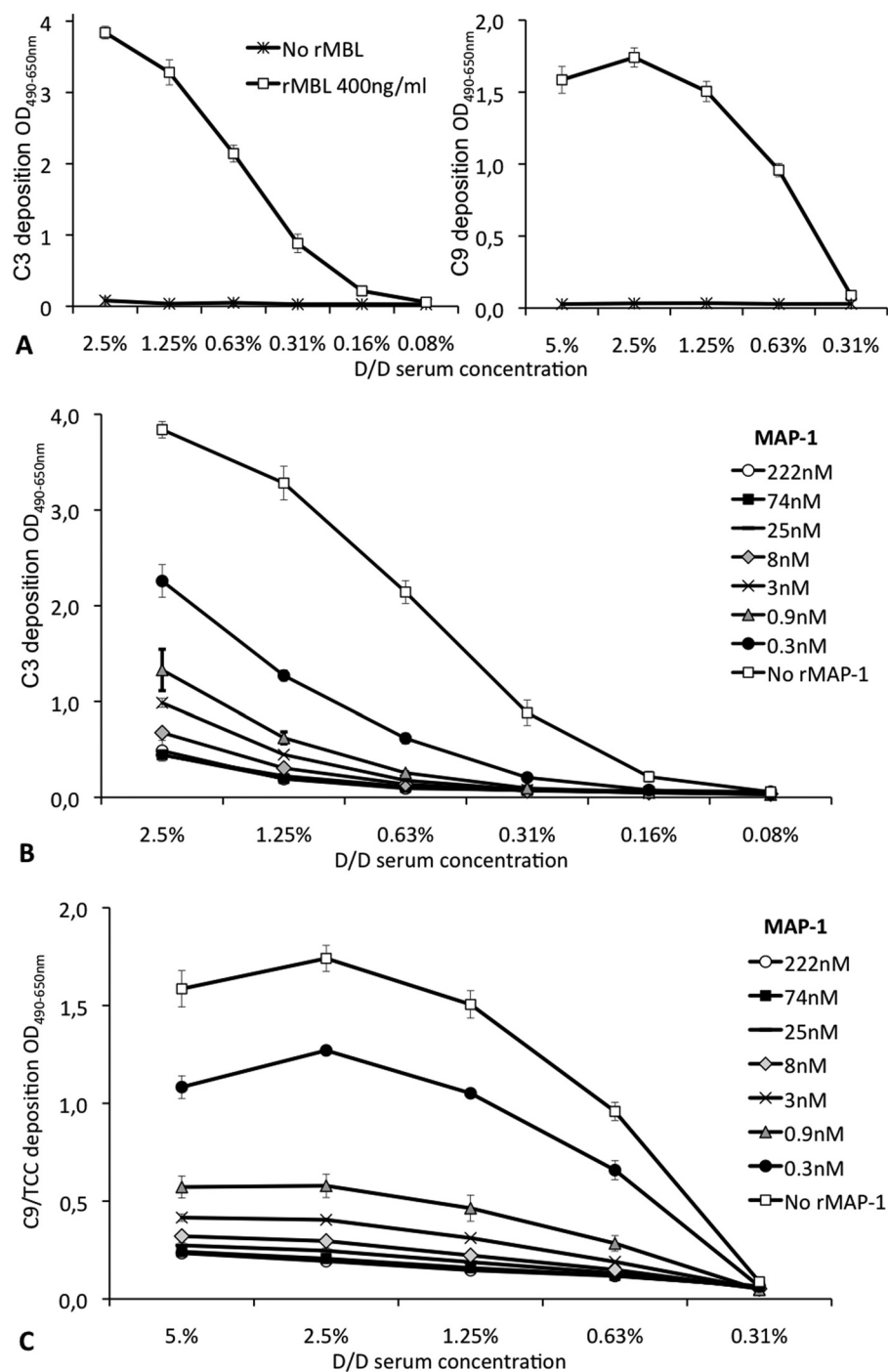


FIGURE 6. **Complement inhibition of MAP-1.** *A*, shown is dose-dependent deposition of C3 (*left*) and C9 (*right*) on solid phase mannan. Serum from a homozygous D/D MBL defect serum  $\pm$  reconstitution with  $0.4 \mu\text{g/ml}$  recombinant MBL preincubated on the mannan-coated wells is shown. *B* and *C*, dose-dependent MAP-1 inhibition of the MBL-dependent activation and deposition of C3 (*B*) and C9/terminal complement complex (*C*) is shown. rMBL at a concentration of  $400 \text{ ng/ml}$  was applied to mannan-coated microtiter plates followed by incubation with serial dilutions of rMAP-1. MBL defect serum of the D/D genotype (serum concentrations are shown in the *x* axis) was subsequently incubated with the MBL/MAP-1 complexes, and the activation and deposition of endogenous C3 or C9 were measured with specific monoclonal antibodies. The different curves illustrate the dose-dependent MAP-1 inhibition of the MBL-dependent activation and deposition of C3. Error bars indicate two times the S.D. of double determinations.

$\sim 330 \text{ \AA}$ . This distance is slightly larger than the span of the lectin heads in the multimeric bunch-like ficolins as imaged by electron microscopy ( $200\text{--}250 \text{ \AA}$ ) (34, 35), implying that once the MASP-1 dimer associates with the ficolin multimer, even if the center of the dimer were to be buried inside the ficolin bunch, the MASP-1 serine protease domains would protrude

from the complex, ready to interact with and cleave its substrate.

MAP-1 has previously been described as a homo-tetramer determined by gel filtration approaches (22). Initially we also examined the rMAP-1 mass by size exclusion chromatography on a Superdex 200 column. Based on the calculations from the



## Structure and Function of MAP-1

molecular mass index standard, we found an apparent molecular size peak of 250 kDa corresponding roughly to a homopenta or a hexamer under physiological calcium conditions. The peak shifted in the absence of calcium and was estimated to ~80 kDa or roughly a dimer (data not shown). We used multi-angle laser light scattering to determine accurate molecular masses under physiological and calcium-free conditions. Multi-angle laser light scattering yielded mass determinations of 94 kDa in the presence of calcium and around 47 kDa when calcium was chelated by EDTA and thus confirmed the expected calcium-dependent homo-dimerization described previously for the MASPs (16, 25, 33, 36).

We previously assessed the serum associations of MAP-1 and MASP-3 with the ficolins and MBL with different immunoprecipitation strategies and ELISA setups (16, 23, 24). Here we measured the direct interactions between recombinant MAP-1 or MASP-3 with MBL and ficolin-3 using surface plasmon resonance spectroscopy. As for earlier studies of proteins containing the CUB<sub>1</sub>-EGF-CUB<sub>2</sub> domains (31–33), we measured affinities on the order of ~5 nM, implying that the domains differing between these proteins have no or minimal impact on the affinity with which they interact with their ligand partner.

We assessed the C3 and C9 complement activation and deposition on mannan by reconstitution of homozygous MBL defect serum with recombinant MBL. When mannan-bound rMBL was preincubated with rMAP-1 in different dilutions (0.3–222 nM), we observed a marked concentration-dependent inhibition of both C3 and C9. Complement inhibition was seen already from a concentration of 0.3 nM and reached an almost complete inhibition plateau around 8 nM. The relatively low MAP-1 concentration required for complement inhibition indicates that ligand-bound MBL provides a much better contact surface for the MAP-1 molecule compared with directly immobilized (and presumably partial denatured) MBL on a biacore chip, where we observed a  $K_d$  of around 5 nM. This may also imply that the actual affinity/avidity *in vivo* could be much greater than observed in the different *in vitro* setups. MAP-1 has previously been shown to down-regulate the C4 activation *in vitro* in the lectin complement pathway; however, accumulating evidence suggests that the MASPs and in particular MASP-1 are involved in different steps of the coagulation cascade (18, 37–40), and MAP-1 could be a putative modulator of that cascade as well. In addition, two independent genetic studies have shown that mutations in the exons encoding the serine protease of MASP-3 influence tissue and bone morphogenesis and give rise to developmental disorders (20, 21). Although the MASP-3 substrate and functions behind these observations remain to be established, the homology between MAP-1 and MASP-3 may imply that MAP-1 holds an additional role as a regulator in tissue development. We further investigated the individual components by co-incubation MAP-1 and the three MASPs on a ficolin-3 ligand matrix, allowing the molecules to compete directly for the association with ficolin-3.

In excess molar concentrations we found that rMAP-1 was able to block the MASP binding to ficolin-3 when MAP-1/MASP was applied simultaneously. This may imply that although MAP-1 appears to circulate in lower systemic concentrations than the MASPs (16, 24, 41, 42), a high local MAP-1

concentrations *in vivo* (e.g. in inflamed tissues) could be an important factor that regulates the MASP activity and attenuates tissue damage driven by complement and perhaps also coagulation activity.

In conclusion, we introduce the first crystal structure of the MBL/ficolin-associated protein-1 (MAP-1), a modulating protein of the lectin complement pathway, and show that the molecule blocks the ligand binding of all three MASPs and mediates a significant down-regulating effect on the complement activation, evaluated as deposition of the central factor C3 and the major terminal complement component C9.

## REFERENCES

- Walport, M. J. (2001) Complement. Second of two parts. *N. Engl. J. Med.* **344**, 1140–1144
- Walport, M. J. (2001) Complement. First of two parts. *N. Engl. J. Med.* **344**, 1058–1066
- Zipfel, P. F., and Skerka, C. (2009) Complement regulators and inhibitory proteins. *Nat. Rev. Immunol.* **9**, 729–740
- Zipfel, P. F. (2001) Complement factor H. physiology and pathophysiology. *Semin. Thromb. Hemost.* **27**, 191–199
- Rasmussen, J. M., Teisner, B., Brandt, J., Brandslund, I., and Gry, H. (1990) Metabolism of C3 and factor B in patients with congenital factor I deficiency. *J. Clin. Lab. Immunol.* **31**, 59–67
- Møller Rasmussen, J., Teisner, B., Jepsen, H. H., Svehag, S. E., Knudsen, F., Kirstein, H., and Buhl, M. (1988) Three cases of factor I deficiency. The effect of treatment with plasma. *Clin. Exp. Immunol.* **74**, 131–136
- Busche, M. N., Pavlov, V., Takahashi, K., and Stahl, G. L. (2009) Myocardial ischemia and reperfusion injury is dependent on both IgM and mannose-binding lectin. *Am. J. Physiol. Heart Circ. Physiol.* **297**, H1853–H1859
- Busche, M. N., Walsh, M. C., McMullen, M. E., Guikema, B. J., and Stahl, G. L. (2008) Mannose-binding lectin plays a critical role in myocardial ischaemia and reperfusion injury in a mouse model of diabetes. *Diabetologia* **51**, 1544–1551
- de Vries, B., Walter, S. J., Peutz-Kootstra, C. J., Wolfs, T. G., van Heurn, L. W., and Buurman, W. A. (2004) The mannose-binding lectin-pathway is involved in complement activation in the course of renal ischemia-reperfusion injury. *Am. J. Pathol.* **165**, 1677–1688
- Garred, P., Honoré, C., Ma, Y. J., Munthe-Fog, L., and Hummelshøj, T. (2009) MBL2, FCN1, FCN2 and FCN3-The genes behind the initiation of the lectin pathway of complement. *Mol. Immunol.* **46**, 2737–2744
- Turner, M. W. (2003) The role of mannose-binding lectin in health and disease. *Mol. Immunol.* **40**, 423–429
- Endo, Y., Matsushita, M., and Fujita, T. (2007) Role of ficolin in innate immunity and its molecular basis. *Immunobiology* **212**, 371–379
- Fujita, T. (2002) Evolution of the lectin-complement pathway and its role in innate immunity. *Nat. Rev. Immunol.* **2**, 346–353
- Thiel, S., Vorup-Jensen, T., Stover, C. M., Schwaebler, W., Laursen, S. B., Poulsen, K., Willis, A. C., Eggleton, P., Hansen, S., Holmskov, U., Reid, K. B., and Jensenius, J. C. (1997) A second serine protease associated with mannan-binding lectin that activates complement. *Nature* **386**, 506–510
- Takahashi, M., Iwaki, D., Kanno, K., Ishida, Y., Xiong, J., Matsushita, M., Endo, Y., Miura, S., Ishii, N., Sugamura, K., and Fujita, T. (2008) Mannose-binding lectin (MBL)-associated serine protease (MASP)-1 contributes to activation of the lectin complement pathway. *J. Immunol.* **180**, 6132–6138
- Skjoedt, M. O., Palarasah, Y., Munthe-Fog, L., Jie Ma, Y., Weiss, G., Skjoedt, K., Koch, C., and Garred, P. (2010) MBL-associated serine protease-3 circulates in high serum concentrations predominantly in complex with Ficolin-3 and regulates Ficolin-3-mediated complement activation. *Immunobiology* **215**, 921–931
- Takahashi, M., Ishida, Y., Iwaki, D., Kanno, K., Suzuki, T., Endo, Y., Homma, Y., and Fujita, T. (2010) Essential role of mannose-binding lectin-associated serine protease-1 in activation of the complement factor D. *J. Exp. Med.* **207**, 29–37
- Krurup, A., Gulla, K. C., Gál, P., Hajela, K., and Sim, R. B. (2008) The action



- of MBL-associated serine protease 1 (MASP1) on factor XIII and fibrinogen. *Biochim. Biophys. Acta* **1784**, 1294–1300
19. Dobó, J., Major, B., Kékesi, K. A., Szabó, I., Megyeri, M., Hajela, K., Juhász, G., Závodszy, P., and Gál, P. (2011) Cleavage of kininogen and subsequent bradykinin release by the complement component. Mannose-binding lectin-associated serine protease (MASP)-1. *PLoS One* **6**, e20036
  20. Rooryck, C., Diaz-Font, A., Osborn, D. P., Chabchoub, E., Hernandez-Hernandez, V., Shamseldin, H., Kenny, J., Waters, A., Jenkins, D., Kaissi, A. A., Leal, G. F., Dallapiccola, B., Carnevale, F., Bitner-Glindzicz, M., Lees, M., Hennekam, R., Stanier, P., Burns, A. J., Peeters, H., Alkuraya, F. S., and Beales, P. L. (2011) Mutations in lectin complement pathway genes COLEC11 and MASP1 cause 3MC syndrome. *Nat. Genet.* **43**, 197–203
  21. Sirmaci, A., Walsh, T., Akay, H., Spiliopoulos, M., Sakalar, Y. B., Hasanefendiolu-Bayrak, A., Duman, D., Farooq, A., King, M. C., and Tekin, M. (2010) MASP1 mutations in patients with facial, umbilical, coccygeal, and auditory findings of Carnevale, Malpuech, OSA, and Michels syndromes. *Am. J. Hum. Genet.* **87**, 679–686
  22. Degn, S. E., Hansen, A. G., Steffensen, R., Jacobsen, C., Jensenius, J. C., and Thiel, S. (2009) MAP44, a human protein associated with pattern recognition molecules of the complement system and regulating the lectin pathway of complement activation. *J. Immunol.* **183**, 7371–7378
  23. Skjoedt, M. O., Hummelshoj, T., Palarasah, Y., Honore, C., Koch, C., Skjodt, K., and Garred, P. (2010) A novel mannose-binding lectin/ficolin-associated protein is highly expressed in heart and skeletal muscle tissues and inhibits complement activation. *J. Biol. Chem.* **285**, 8234–8243
  24. Skjoedt, M. O., Hummelshoj, T., Palarasah, Y., Hein, E., Munthe-Fog, L., Koch, C., Skjodt, K., and Garred, P. (2011) Serum concentration and interaction properties of MBL/ficolin-associated protein-1. *Immunobiology* **216**, 625–632
  25. Teillet, F., Gaboriaud, C., Lacroix, M., Martin, L., Arlaud, G. J., and Thielens, N. M. (2008) Crystal structure of the CUB1-EGF-CUB2 domain of human MASP-1/3 and identification of its interaction sites with mannan-binding lectin and ficolins. *J. Biol. Chem.* **283**, 25715–25724
  26. Gál, P., Dobó, J., Závodszy, P., and Sim, R. B. (2009) Early complement proteases: C1r, C1s, and MASPs. A structural insight into activation and functions. *Mol. Immunol.* **46**, 2745–2752
  27. Vorup-Jensen, T., Sørensen, E. S., Jensen, U. B., Schwaeble, W., Kawasaki, T., Ma, Y., Uemura, K., Wakamiya, N., Suzuki, Y., Jensen, T. G., Takahashi, K., Ezekowitz, R. A., Thiel, S., and Jensenius, J. C. (2001) Recombinant expression of human mannan-binding lectin. *Int. Immunopharmacol.* **1**, 677–687
  28. Palarasah, Y., Nielsen, C., Sprogøe, U., Christensen, M. L., Lillevang, S., Madsen, H. O., Bygum, A., Koch, C., Skjodt, K., and Skjoedt, M. O. (2011) Novel assays to assess the functional capacity of the classical, the alternative and the lectin pathways of the complement system. *Clin. Exp. Immunol.* **164**, 388–395
  29. Palarasah, Y., Skjoedt, M. O., Vitved, L., Andersen, T. E., Skjoedt, K., and Koch, C. (2010) Sodium polyanethole sulfonate as an inhibitor of activation of complement function in blood culture systems. *J. Clin. Microbiol.* **48**, 908–914
  30. Garred, P., Larsen, F., Madsen, H. O., and Koch, C. (2003) Mannose-binding lectin deficiency revisited. *Mol. Immunol.* **40**, 73–84
  31. Cseh, S., Vera, L., Matsushita, M., Fujita, T., Arlaud, G. J., and Thielens, N. M. (2002) Characterization of the interaction between L-ficolin/p35 and mannan-binding lectin-associated serine proteases-1 and -2. *J. Immunol.* **169**, 5735–5743
  32. Teillet, F., Dublet, B., Andrieu, J. P., Gaboriaud, C., Arlaud, G. J., and Thielens, N. M. (2005) The two major oligomeric forms of human mannan-binding lectin. Chemical characterization, carbohydrate-binding properties, and interaction with MBL-associated serine proteases. *J. Immunol.* **174**, 2870–2877
  33. Zundel, S., Cseh, S., Lacroix, M., Dahl, M. R., Matsushita, M., Andrieu, J. P., Schwaeble, W. J., Jensenius, J. C., Fujita, T., Arlaud, G. J., and Thielens, N. M. (2004) Characterization of recombinant mannan-binding lectin-associated serine protease (MASP)-3 suggests an activation mechanism different from that of MASP-1 and MASP-2. *J. Immunol.* **172**, 4342–4350
  34. Ohashi, T., and Erickson, H. P. (1998) Oligomeric structure and tissue distribution of ficolins from mouse, pig, and human. *Arch. Biochem. Biophys.* **360**, 223–232
  35. Gout, E., Moriscot, C., Doni, A., Dumestre-Pérard, C., Lacroix, M., Pérard, J., Schoehn, G., Mantovani, A., Arlaud, G. J., and Thielens, N. M. (2011) M-ficolin interacts with the long pentraxin PTX3. A novel case of cross-talk between soluble pattern-recognition molecules. *J. Immunol.* **186**, 5815–5822
  36. Thielens, N. M., Cseh, S., Thiel, S., Vorup-Jensen, T., Rossi, V., Jensenius, J. C., and Arlaud, G. J. (2001) Interaction properties of human mannan-binding lectin (MBL)-associated serine proteases-1 and -2, MBL-associated protein 19, and MBL. *J. Immunol.* **166**, 5068–5077
  37. Krarup, A., Wallis, R., Presanis, J. S., Gál, P., and Sim, R. B. (2007) Simultaneous activation of complement and coagulation by MBL-associated serine protease 2. *PLoS ONE* **2**, e623
  38. La Bonte, L. R., Pavlov, V. I., Tan, Y. S., Takahashi, K., Takahashi, M., Banda, N. K., Zou, C., Fujita, T., and Stahl, G. L. (2012) Mannose-binding lectin-associated serine protease-1 is a significant contributor to coagulation in a murine model of occlusive thrombosis. *J. Immunol.* **188**, 885–891
  39. Gulla, K. C., Gupta, K., Krarup, A., Gal, P., Schwaeble, W. J., Sim, R. B., O'Connor, C. D., and Hajela, K. (2010) Activation of mannan-binding lectin-associated serine proteases leads to generation of a fibrin clot. *Immunology* **129**, 482–495
  40. Takahashi, K., Chang, W. C., Takahashi, M., Pavlov, V., Ishida, Y., La Bonte, L., Shi, L., Fujita, T., Stahl, G. L., and Van Cott, E. M. (2011) Mannose-binding lectin and its associated proteases (MASPs) mediate coagulation and its deficiency is a risk factor in developing complications from infection, including disseminated intravascular coagulation. *Immunobiology* **216**, 96–102
  41. Møller-Kristensen, M., Jensenius, J. C., Jensen, L., Thielens, N., Rossi, V., Arlaud, G., and Thiel, S. (2003) Levels of mannan-binding lectin-associated serine protease-2 in healthy individuals. *J. Immunol. Methods* **282**, 159–167
  42. Terai, I., Kobayashi, K., Matsushita, M., and Fujita, T. (1997) Human serum mannan-binding lectin (MBL)-associated serine protease-1 (MASP-1). Determination of levels in body fluids and identification of two forms in serum. *Clin. Exp. Immunol.* **110**, 317–323